Impact of the Desilication Treatment of Y Zeolite on the Catalytic Cracking of Bulky Hydrocarbon Molecules

Juan Rafael García, Marisa Falco & Ulises Sedran

Topics in Catalysis

ISSN 1022-5528

Top Catal
DOI 10.1007/s11244-015-0432-7

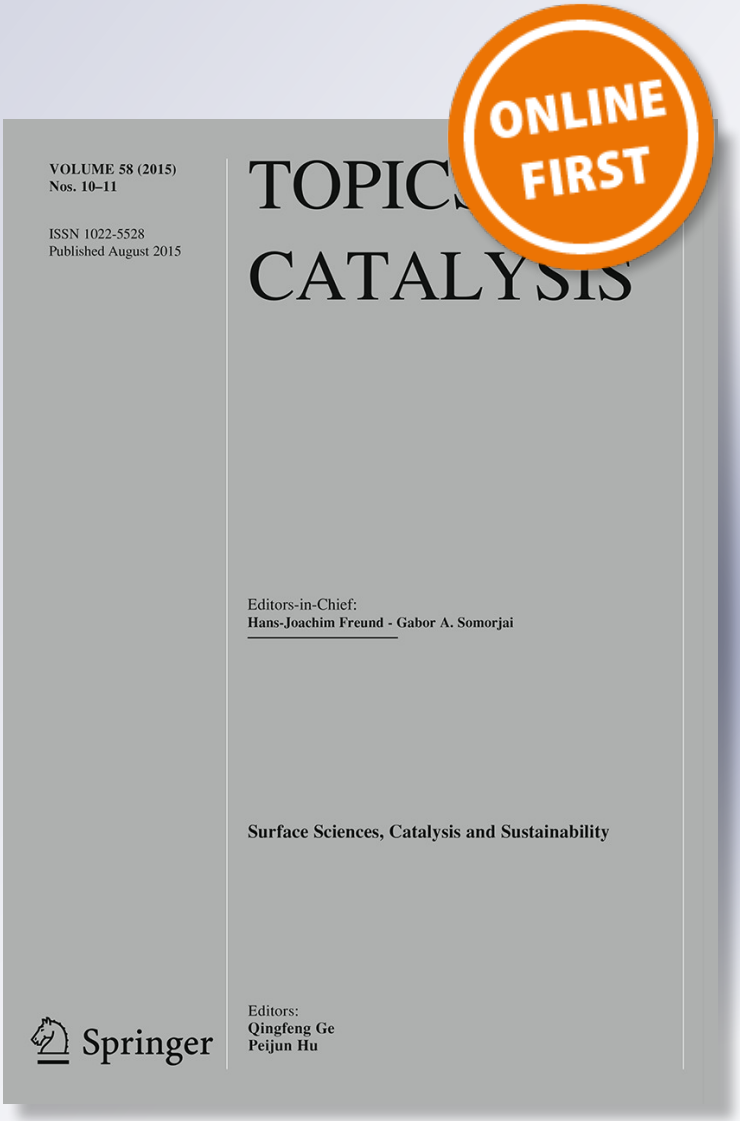

Springer

Top Catal
DOI 10.1007/s11244-015-0432-7

ORIGINAL PAPER

Impact of the Desilication Treatment of Y Zeolite on the Catalytic Cracking of Bulky Hydrocarbon Molecules

Juan Rafael García[1] · **Marisa Falco**[1] · **Ulises Sedran**[1]

Abstract Mesoporosity was induced on a USY zeolite by means of an alkaline leaching process. Samples were immersed in 0.05, 0.10 and 0.20 M NaOH solutions during 15 min at room temperature and then were exchanged with NH_4^+ ions and calcined to yield the acid forms. The formation of mesopores with size ranging from 20 to 100 Å increased with the concentration of NaOH. The modified zeolites were used at 30 wt% to formulate cracking catalysts with an inert SiO_2 matrix. The catalytic performance of these catalysts in the conversion of 1,3,5-tri-isopropylbenzene was evaluated in a batch, fluidized bed reactor at 450, 500 and 530 °C, with a catalyst to oil relationship of 4.7 and contact times up to 16 s. The catalysts with the modified zeolites were more active in the cracking of these bulky molecules than the one with the parent, unmodified zeolite; moreover, the selectivity to the products of primary cracking reactions increased. These results reveal an enhanced diffusion of the reactant molecules to the zeolite active sites and of the products out of the catalyst particles.

Keywords Mesopore · Zeolite · Desilication · Diffusion · Cracking selectivity

✉ Ulises Sedran
usedran@fiq.unl.edu.ar

[1] Instituto de Investigaciones en Catálisis y Petroquímica INCAPE (FIQ, UNL –CONICET), Colectora Ruta Nac. N° 168 km 0 - Paraje El Pozo, 3000 Santa Fe, Argentina

1 Introduction

The process of catalytic cracking of hydrocarbons (FCC) is one of the most important and profitable to produce different fuels such as gasoline and middle distillates and petrochemical raw materials in current refineries [1]. Among most significant stressing issues, the worldwide increasing demand for diesel fuel and petrochemical raw materials and the rising use of different residual feedstocks in the last decade [2] must be mentioned. Resids have higher contents of contaminant metals, polynuclear aromatics, heteroatoms and complex macromolecular groups than standard hydrocarbon feedstocks [3], which are typically vacuum gas oils (VGO). This represents an important challenge for FCC technology, and improvements in the transport properties of the commercial catalysts would be attractive in order to improve the selectivity to desired products and decrease undesired secondary reactions [4–8].

The diffusion restrictions in Y zeolite micropores could be decreased following three different approaches [8]. The first one consists in synthesizing zeolites with extra-large pores [9] which, however, would show a different topology and low hydrothermal stability. The second one is based on the use of smaller Y zeolite crystal size, so as to increase the external specific surface area and decrease diffusion paths in the crystals [4, 5, 10]. A third possibility is the induction of intracrystalline mesopores, that is, cracks, cavities [11] and cylindrical channels [12] in the crystals in the mesopore size range, that are interconnected in a wormhole-like manner to each other [8].

This last approach can be performed by means of different ways [13], among which desilication has been extensively applied to ZSM-5 [8, 11, 14] and, in the last years, to Y zeolite [6, 13, 15–17]. The treatment consists in the alkaline leaching which removes silicon atoms from the

Published online: 06 August 2015

zeolite crystalline network, thus inducing the partial destruction of the network and consequently being the origin of mesoporosity [8]. If conditions are appropriate, it is possible to attain a catalyst with the desired activity and selectivity in the micropores and intracrystalline mesopores helping reactants and products to diffuse more easily [18]. As an example, Groen et al. [19] showed that the neopentane characteristic diffusion time (L^2/D) in desilicated ZSM-5 can be two orders of magnitude shorter than in the reference, unmodified microporous zeolite; the authors concluded that an interconnected mesoporous system was formed.

Commercial FCC catalysts are composed, with Y zeolite as the main component supported on a matrix, which can be either active or inactive, plus binder, filler and, usually, various additives with different roles. The catalyst particle size is typically 70 μm average and the zeolite crystals are below 1 μm [4, 20]. Most of the active sites are located in the zeolite internal micropore structure and, then, it is necessary that reactant molecules be able to diffuse in this porous system in order to reach the active sites, adsorb and react. As in all catalytic system, both chemical (acidity) and porous structure do have an impact on the performance of FCC catalysts but, particularly, bulky molecules, whose critical diameters are larger than the micropore size in Y zeolite, such as those found in FCC feedstocks, would hardly access internal sites, being subjected to serious diffusion restrictions in the catalyst pore system [4–8, 21, 22]. These molecules could crack on the matrix, if active, or the external sites in the zeolite crystals.

1,3,5-Tri-isopropylbenzene (TIPB), its molecules having a critical diameter of 9.5 Å [4], has been used as a model compound in the study of diffusion–reaction phenomena in FCC catalysts. For example, accessibility in FCC matrices [23], impact of the different size in Y zeolite particles [4, 5, 24], and various issues in acidic catalysts [10, 21, 25]. Most important positive characteristics are that the molecules' critical diameter is significantly larger than the Y zeolite pore size (7.4 Å), and its reaction can be tracked relatively easily, since the cracking reaction follows a basically sequential path of the scission of the side alkyl chains while the benzenic ring keeps essentially unaltered [4, 21, 23]. It is precisely this well known mechanism which allows observing product distributions under a kinetic approach considering the influence of diffusion restrictions on primary and secondary cracking [26].

It is the objective of this work to evaluate the impact of mesoporosity generated by alkaline desilication treatment over the Y zeolite component of FCC catalysts on the catalytic cracking of 1,3,5-tri-isopropylbenzene taken as a model compound representative of bulky molecules in FCC systems.

2 Experimental

2.1 Zeolite Alkaline Leaching (Desilication)

Mesoporosity was induced on the crystals of Y zeolite by means of the following alkaline lixiviation procedure [13, 17]. Various portions of a commercial Y zeolite (Zeolyst CBV 760, Si/Al = 30, H-form) were immersed in NaOH aqueous solutions at 1 g zeolite/30 mL, the concentrations being 0.05, 0.10 and 0.20 M, and kept under stirring at 25 °C during 15 min. After that, the suspensions were neutralized with an HCl 1.00 M solution. These zeolites were exchanged three times with 0.50 M NH_4Cl (Carlo Erba, 99.5 %) solutions, at 1 g zeolita/5 mL solution, and then thoroughly washed with deionized water, dried at 110 °C during 16 h and finally calcined at 550 °C during 4 h to have the zeolites in their protonic form. The zeolites were named Z-00 (no treatment), Z-05, Z-10 and Z-20, in consistency with the NaOH concentration in the treating solutions.

2.2 Zeolite Characterization

Zeolite X-ray diffraction patterns were collected in a Shimadzu XD-D1 diffractometer in the $5° < 2\theta < 40°$ range. Unit cell sizes (UCS) were calculated according to the ASTM D 3942 method. The degrees of crystallinity were calculated according to the ASTM D 3906 method; the areas of the 331, 511, 440, 533, 642, 660, 555 and 664 reflections peaks were used to estimate the relative crystallinity for the various samples in reference to the parent zeolite Z-00, which was assigned 100 % crystallinity.

The textural properties were determined by means of the adsorption of nitrogen at −196 °C in a Quantachrome Autosorb-1 sorptometer. The samples were previously degassed at 300 °C during 3 h. The specific surface area was assessed following the BET method in the $0.15 < P/Po < 0.30$ range, the total pore volume was estimated at $P/Po \sim 0.98$ and the micropore volume and the specific surface area of the mesopores were estimated with the *t*-plot method in the $3.5 \text{ Å} < t < 5.0 \text{ Å}$ range. The mesopore size distribution was assessed with the Barrett-Joyner-Halenda (BJH) model.

The nature, amount and strength of acidic sites in the different zeolites were determined by means of the FTIR analysis of adsorbed pyridine (Merck, 99.5 %) as a probe molecule in a Shimadzu FTIR Prestige-21 equipment. Approximately 100 mg of the zeolites were pressed at 1 ton/cm^2 in order to produce self supporting wafers with density 440 g/m^2, which were then placed into a cell with CaF_2 windows. Samples were initially degassed at 450 °C during 2 h and a background spectrum was collected at

room temperature. Pyridine adsorption was performed at room temperature and after successive desorptions at 150, 300 and 400 °C, spectra were recorded at room temperature with a resolution of 4 cm^{-1} at pressure of 10^{-4} Torr. The amounts of Brönsted and Lewis acid sites were calculated from the integrated absorbance of the bands at 1545 and 1450–1460 cm^{-1}, respectively, by means of the integrated molar extinction coefficients, which are considered independent from the catalyst and site strength [27, 28].

The elemental composition of the parent and modified zeolites was determined by the inductively coupled plasma (ICP) technique, using a Perkin-Elmer Optical Emission Spectrometer OPTIMA 2100 DV.

2.3 Evaluation of the Catalytic Performance

The zeolite samples were steamed (100 % steam) at 788 °C during 5 h in order to stabilize them. The catalysts were prepared by adding the previously desilicated Y zeolites to an essentially inactive matrix (mesoporous silica, chromatographic grade, Merck) and a colloidal silica binder (Ludox AS-40, Aldrich) [17]. The zeolite, the matrix and the binder were added at 30, 50 and 20 wt%, respectively, to form the catalysts, reproducing typical formulations of the catalysts used in the FCC process [5, 10]. Finally, the catalysts were dried at 110 °C during 16 h and calcined in an oven at 550 °C during 4 h in air. The solids were grounded and sieved to the 75–125 μm range. The catalysts were named Cat-00, Cat-05, Cat-10 and Cat-20, following the nomenclature of the corresponding zeolites.

The experiments of 1,3,5-tri-isopropylbenzene (Aldrich, 95 %) conversion were performed in a CREC Riser Simulator reactor, which is a batch, fluidized bed laboratory reactor which closely mimics the conditions of the commercial FCC process [29]. The unit has been described comprehensively elsewhere [30, 31]. Reaction times in the experiments were from 4, 8, 12 and 16 s, temperature was 500 °C and catalyst to oil relationship was 4.7. The mass of catalyst was 0.4 g and the volume of TIPB injected was 0.1 ml in all the cases. Experiments of purely thermal cracking, with no catalyst in the reactor, were performed at the same temperature and the longest contact time. Experiments with catalysts Cat-00, Cat-10 and Cat-20 were also performed at 450 and 530 °C. The reaction products were analyzed by on-line standard capillary gas chromatography, using a 30 m long, 250 μm diameter and 0.25 μm film thickness, non-polar, dimethylpolysiloxane column. Product identification was performed with the help of standards and GC–MS analysis. The coke content was assessed by means of a method with temperature-programmed oxidation and further methanation of the carbon oxides over a Ni catalyst, quantified with the help of a FID detector. Mass balances (recoveries) closed to more than 90 % in all the cases.

3 Results and Discussion

3.1 Resulting Zeolite Properties

Table 1 shows the textural properties of the parent zeolite and the modified samples. It can be seen that the higher the concentration of alkali during the lixiviation, the more important the increase of mesoporosity in the zeolites. For example, the specific surface area of mesopores in the parent zeolite increased 60 % in the sample treated with NaOH 0.10 M and doubled in the sample treated with NaOH 0.20 M. The volumes of mesopores also showed the same trend.

Figure 1 shows the mesopore size distribution (BJH) of the parent and the desilicated zeolites, which are in line with the other properties shown in Table 1 and, moreover, indicate that the new mesopores have increasingly larger average sizes.

Figure 2 shows the X-ray diffraction patterns of the various samples. It can be seen that the intensity of the peaks decreased as a function of the increasing severity of the treatment. This is also confirmed by the crystallinity of the zeolites which are shown in Table 2 in reference to the parent zeolite (Z-00). Similar results in relation to the loss of crystallinity in the Y zeolites after alkaline lixiviation were reported by Verboekend et al. [15]. The sizes of the unit cells increased slightly with the desilication treatment (refer to Table 2), but they were overall small, in the 24.23–24.26 Å range. Rigorous studies with different zeolite structures showed that when alkaline desilication is performed with the help of organic pore-directing agents such as tetraalkylammonium hydroxides, the Si/Al relationship is maintained and, to a great extent, also the crystallinity of the parent zeolite. But if the process is carried out without pore-directing agents, a selective removal of silicon atoms from the zeolite framework will occur [15]. The slight increase in UCS is the consequence of the selective extraction of silicon atoms, since the length of Si–O bonds in the zeolite framework is shorter than that of the Al–O bonds, thus producing a larger size of the unit cells. However, while the framework Si/Al decreases according to the severity of the desilication treatment, as shown by the increasing UCSs, the bulk Si/Al relationship is essentially constant (about 23), thus suggesting that silicon atoms are removed selectively from the zeolite crystals and would end up as amorphous extraframework species.

The parent zeolite Z-00 was originally in the protonic form and the desilicated samples were submitted to three

Table 1 Textural properties of the parent zeolite and desilicated samples

	Z-00	Z-05	Z-10	Z-20
BET specific surface area (m^2/g)	838	835	828	724
Mesopore specific surface area (m^2/g)	226	358	366	454
Total pore volume (cm^3/g)	0.632	0.659	0.686	0.810
Mesopore volume (cm^3/g)[a]	0.282	0.387	0.420	0.652

[a] Mesopore volume = total pore volume−micropore volume

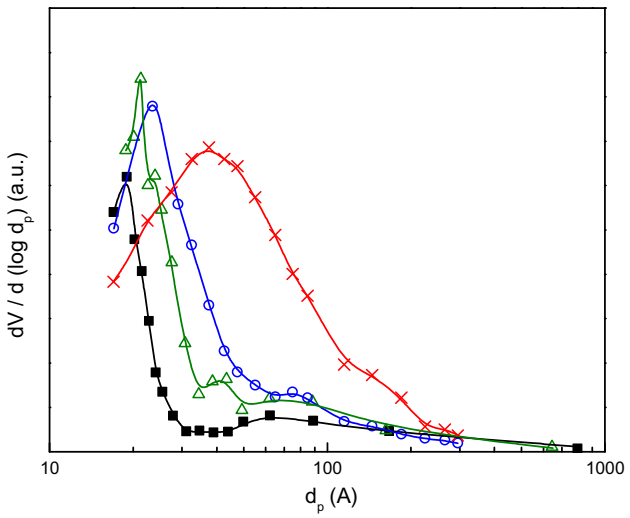

Fig. 1 Mesopore size distributions (BJH) of the parent and the desilicated zeolites. Symbols: *square* Z-00, *triangle* Z-05, *circle* Z-10, *cross mark* Z-20

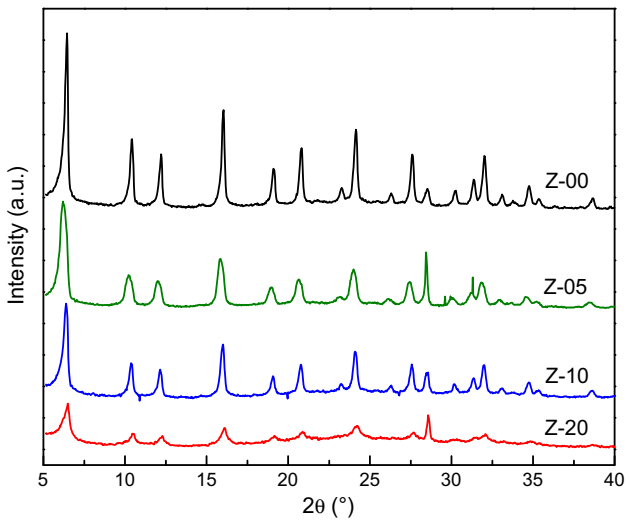

Fig. 2 X-ray diffraction patterns of the parent and the desilicated zeolites

Table 2 Crystalline properties of the parent zeolite and desilicated samples

	Z-00	Z-05	Z-10	Z-20
Cristallinity (%)	100	75	66	54
UCS (Å)	24.23	24.24	24.25	24.26

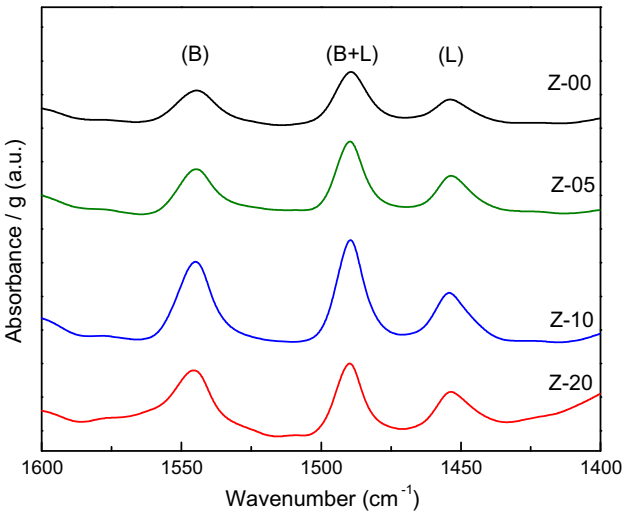

Fig. 3 FTIR spectra of pyridine adsorbed at room temperature and evacuated at 150 °C over the parent and the desilicated zeolites

Table 3 Distributions of acid sites (pyridine FTIR; μmol/g; B: Brönsted and L: Lewis sites) in the parent zeolite and desilicated samples

Sample	Temperature (°C)					
	150 °C		300 °C		400 °C	
	B	L	B	L	B	L
Z-00	60	23	53	15	21	16
Z-05	69	34	50	15	30	14
Z-10	126	49	83	40	30	27
Z-20	73	41	52	23	23	21

steps of ion exchange with ammonium salts after the treatment; further, they were calcined to recover the acidic form. Figure 3 shows the example of FTIR pyridine absorption spectra gathered after desorption at 150 °C, while Table 3 shows the amount of Brönsted and Lewis sites after desorption at 150, 300 and 400 °C, respectively.

The amount of acidic sites (mass basis) increased in the zeolites after the different treatments. Both total acidity (as

shown by the lowest desorption temperature 150 °C) and the other ranges of acid strengths manifested this effect, although it was less important in the strong acidic sites. Moreover, the B/L relationship was larger at the lowest desorption temperatures, thus suggesting that the new acidity, which is predominantly Brönsted, has a weaker characteristic. Since the lixiviation process is highly selective to leaching out silica-rich domains [8], aluminium-rich domains and, consequently, tetrahedral Al atoms would remain relatively unchanged, thus producing an increase in acidity on a mass basis. This consequence was especially noted in zeolites Z-05 and Z-10, which did not lose crystallinity severely, differently from zeolite Z-20 (with a larger loss of cristallinity), which showed a smaller increase. Then, given the range of concentrations of the alkaline solutions used in this work, an optimum condition can be defined in reference to the zeolite's acid property.

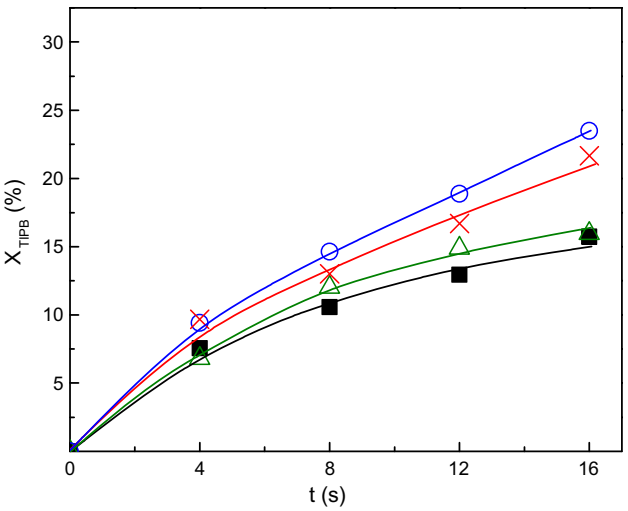

Fig. 4 Conversion of 1,3,5-tri-isopropilbenzene at 500 °C over the parent and the desilicated zeolites. Symbols: *square* Cat-00, *triangle* Cat-05, *circle* Cat-10l, *cross mark* Cat-20

3.2 Catalyst Evaluation

3.2.1 1,3,5-Tri-isopropylbenzene Cracking at 500 °C

Before the catalytic evaluation, the modified zeolites were hydrothermally stabilized by mean of steaming. This process produced loss of crystallinity and specific surface area, which was more intense on the more severely desilicated samples. However, most important properties (average mesopore size, specific surface area, crystallinity, acidity) maintained the trends observed with the zeolites before steaming (values not shown). As discussed, the molecules of 1,3,5-tri-isopropylbenzene, having a critical diameter of 9.5 Å, can be considered relatively bulky, and have been extensively used as a model reactant to reveal diffusion limitations in catalytic cracking catalysts [4, 5, 7, 10, 21–25]. Thermal cracking experiments at 500 °C and 16 s showed that TIPB conversion was 6.6 %, with a compound ($C_{15}H_{22}$) which is a derivative from cadine, with a naphthenic-aromatic structure, being the most important product. In these experiments the cracking products showed a selectivity of only 15 %. It has been reported that $C_{15}H_{22}$ can be easily formed by the effect of temperature [23, 32].

Since both the matrix and the binder in the catalysts are silica, their activity can be assumed to be contributed by the zeolite component only [4, 10, 33]. Figure 4 shows the conversion profiles observed over the four catalysts at 500 °C, where it can be seen that the catalysts with desilicated zeolites all showed to be more active than the one with the parent zeolite Cat-00. Catalyst Cat-05 showed to be slightly more active than Cat-00, thus suggesting that a mild desilication treatment, which produces modest changes in zeolite textural properties and acidity, would then induce moderate improvements in the catalytic performance. However, when the treatments were more severe and modified zeolite properties more extensively, cases of catalysts Cat-10 and Cat-20, they showed appreciably higher conversions, particularly at longer reaction times.

In cracking TIPB on Y zeolite, Morales-Pacheco et al. [24], observed that the smaller the crystal size, the larger the activity, and suggested that it was due to the increase in the external specific surface area of the particles. In the present work, the higher activity in catalysts containing desilicated zeolites could be assigned to the higher accessibility of bulky TIPB molecules to the active sites given by the occurrence of intracrystalline new mesopores. Besides the increased mesoporosity, also acidity showed a positive change, and thus could also contribute to the higher activity exhibited by the catalysts with desilicated zeolites. Catalyst Cat-20 is more active than catalyst Cat-05 even though total acidity was similar on both catalysts (see Table 3). Then, the higher activity in catalyst Cat-20 could be attributed to the higher mesoporosity and better diffusion properties in zeolite Z-20.

Catalyst Cat-10 was the most active in the series, even though the mesoporosity in its zeolite (Z-10) is lower than that of zeolite Z-20 (refer to Fig. 1). This behavior was also observed at 450 and 530 °C, as it will be discussed later. These facts can be rationalized, considering that mesoporosity is high enough in both cases, in the light of the higher acidity of Cat-10.

In all the experiments, the most important reaction products were those from the consecutive cracking of the side chains in the TIPB molecules, that is, 1,3-di-isopropylbenzene (1,3-DIPB), isopropylbenzene (cumene, IPBz), benzene (Bz) and propylene ($C_3^=$); moreover, significant amounts of 1,4-di-isopropylbenzene (1,4-DIPB) and $C_{15}H_{22}$. It is obvious that each cracking step of the

alkyl side chains implies the production of a propylene molecule. Other gases (C_4–), ethylbenzene, n-propylbenzene, 1,3,5-tri-methylbenzene and isobutylbenzene were observed as minor products. Previous reports about the cracking of TIPB over acidic catalysts [4, 5, 22] showed the same main products with the exception of $C_{15}H_{22}$, which was only reported by Falco et al. [23], who observed that the selectivity to this product was high at short reaction times, showing an unstable behavior. 1,4-DIPB, which is always observed with low yields, can be formed by isomerization from 1,3-DIPB, a reaction which occurs easily on acidic catalysts [22]. Besides the three cracking steps of the alkyl side chains, which are clearly dominant, other side reactions leading to minor products in the conversion of TIPB, such as disproportionation, isomerization and condensation [4, 21, 24, 34] have been reported. A very low coke yield, lower than 0.25 wt% was observed in all the cases, in consistency with previous reports about TIPB conversion on FCC catalysts [5] and alumina [23].

Figure 5 shows the yields of the main reaction products as a function of reaction time for catalyst Cat-00, formulated with the parent zeolite, and for catalyst Cat-20, formulated with the most severely treated zeolite. In the case of Cat-00 (Fig. 5a), $C_{15}H_{22}$ was one of the main products at short reaction time, maintaining its yield, while 1,3-DIPB became the most important product at longer reaction times. This initial prevalence of $C_{15}H_{22}$ was also observed on catalysts Cat-05 and Cat-10, but not on Cat-20, as shown in Fig. 5b, where 1,3-DIPB was the most important product from the shortest reaction times.

The yield of 1,3-DIPB can play a main role in the kinetic analysis of the TIPB conversion. In effect, dealkylation of TIPB to yield 1,3-DIPB and $C3^{=}$, 1,3-DIPB dealkylation to yield IPBz and $C3^{=}$, and IPBz dealkylation to yield Bz and $C3^{=}$ is mostly accepted as the main reaction course [4, 5, 21–23]. Then, the yield of 1,3-DIPB is the neat result of both TIPB (primary cracking) and its own dealkylation to IPBz and after that to Bz, both of them defining the secondary cracking. Diffusion restrictions on 1,3-DIPB across the zeolite pore system will increase its residence time in the porous network and, consequently, increase its cracking to IPBz (secondary cracking). The high yield of 1,3-DIPB in catalyst Cat-20 can be understood in the light of this view, since mesoporosity in Z-20 is the highest, thus easing 1,3-DIPB diffusion and decreasing the possibility of its further conversion.

Table 4 shows the selectivities for the main reaction products observed at a given conversion over the desilicated zeolites. It can be seen that the selectivity to the products of primary cracking (1,3-DIPB + 1,4-DIPB, that is, DIPB) increased as a function of zeolite mesoporosity while those of the products of secondary cracking (IPBz and Bz) decreased.

3.2.2 *Effect of the Reaction Temperature*

In order to study the effect of the reaction temperature on the cracking of TIPB molecules, experiments with various catalysts were also performed at 450 and 530 °C. Figure 6 shows the conversion of TIPB as a function of reaction time at the various reaction temperatures, over both the parent Cat-00 (unmodified zeolite) and Cat-10 catalysts; Cat-10 was the most active in the series at all the temperatures. It can be seen that, as expected, conversions increased as a function of reaction temperatures.

Table 4 Selectivities to the products of successive cracking reactions (wt%) of TIPB at 500 °C over the desilicated samples (conversion approximately 14 %)

	Cat-05	Cat-10	Cat-20
DIPB	17.1	30.3	39.3
IPBz	22.2	17.6	15.1
Bz	3.5	1.2	0.6

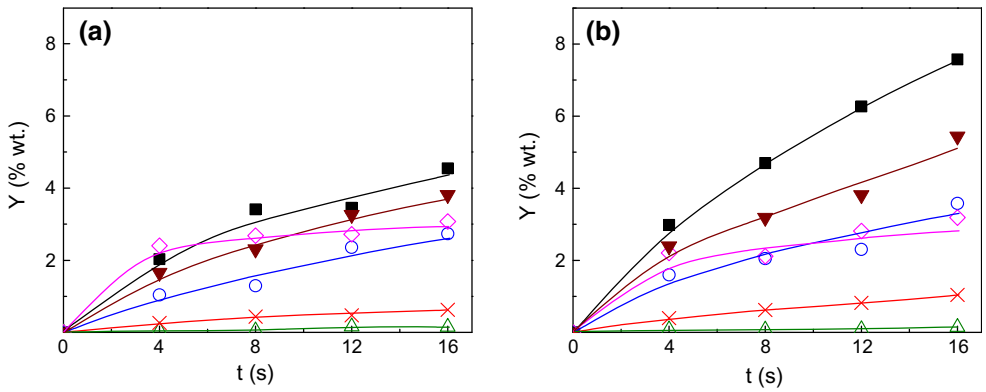

Fig. 5 Yields of the main reaction products as a function of time in the conversion of TIPB at 500 °C **a** Cat-00, **b** Cat-20. Symbols: *square* 1,3-DIPB, *circle* IPBz, *trianle* Bz, *cross mark* 1,4-DIPB, *diamond* $C_{15}H_{22}$, *inverted triangle* $C_3^{=}$

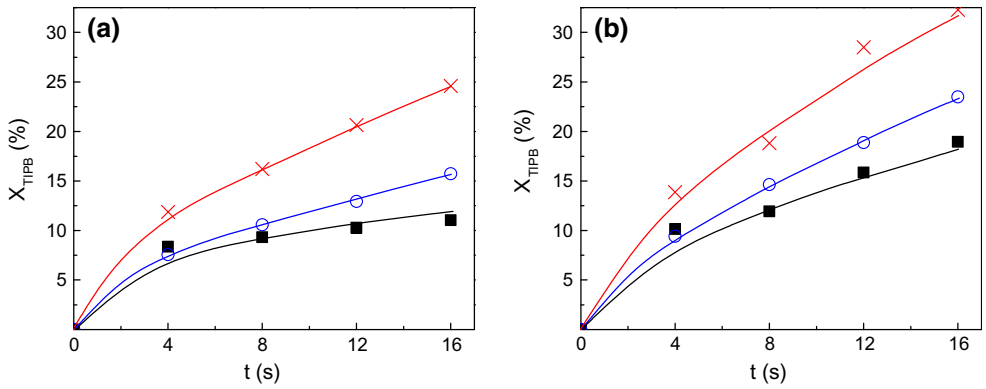

Fig. 6 Conversion of 1,3,5-tri-isopropilbenzene at different temperatures. **a** Cat-00. **b** Cat-10. Symbols: *square* 450 °C, *circle* 500 °C, *cross mark* 530 °C

Table 5 Selectivities to the products of successive cracking reactions (wt%) of TIPB at different temperatures over Cat-10 (conversion approximately 14 %)

	Temperature (°C)		
	450	500	530
DIPB	32.3	30.3	17.2
IPBz	8.9	17.6	19.4
Bz	0.2	1.2	2.1

Table 5 shows the selectivities for the main reaction products observed at a given conversion for the most active catalyst (Cat-10) at different reaction temperatures. It can be seen that the selectivity to the products of primary cracking (1,3-DIPB + 1,4-DIPB) decreased with the temperature while those of the products of secondary cracking (IPBz and Bz) increased. The higher incidence of secondary cracking reactions at higher reaction temperatures can be explained considering the more important impact of temperature on chemical reactions than on diffusion processes, which thus would become more restrictive in the overall diffusion–reaction process rate. In experiments of conversion of TIPB at temperatures between 350 and 500 °C on zeolites which had not an important degree of mesoporosity, the selectivity to IPBz was much higher than that to 1,3-DIPB [4], thus suggesting a much more important occurrence of secondary cracking reactions.

3.2.3 *Impact of Secondary Cracking Reactions. Simple Kinetic Model*

It is well known that diffusion restrictions in the pore system of a catalyst may have a strong impact on the observed activity and product distribution for a given reaction, this issue being particularly important in a set of series reactions [4, 26, 35, 36]. Tauster et al. [26] developed a rigurous method to evaluate diffusion restrictions in a catalyst which promotes a set of reactions where primary and secondary cracking reactions can be identified as following a sequential reaction scheme such as A → B → C. Primary cracking is represented by A → B, and secondary cracking by B → C, where A, B and C are chemical species which do not need to be individual but may be lumps.

As already mentioned, the reaction of TIPB over acidic catalysts can be described by means of three consecutive steps: (a) TIPB dealkylation to 1,3-DIPB, (b) 1,3-DIPB dealkylation to IPBz and (c) IPBz dealkylation to Bz, a molecule of propylene being produced in each of these steps. In the catalytic experiments, other hydrocarbons such as $C_{15}H_{22}$ and 1,4-DIPB, were also observed besides these dealkylation products, as the consequences of side reactions. $C_{15}H_{22}$ can be formed by the cyclization of alkyl groups in the aromatic ring [23, 32], while 1,4-DIPB can be formed from the isomerization of 1,3-DIPB [22]. It can be assumed that the formation of these two hydrocarbons is very fast. Then three lumps in the conversion scheme shown in Fig. 7 can be considered: lump A including TIPB and $C_{15}H_{22}$, lump B including the two DIPB isomers and lump C including cumene and benzene. According to the model by Tauster et al. [26], the conversion of lump A into lump B (where reaction "a" would be the most significant) would be primary cracking, and the conversion of lump B into lump C (where reaction "b" would be the most significant) would be secondary cracking.

In order to produce a selectivity analysis to be applied to the catalytic performances of the various desilicated zeolites with different mesoporosities, a simple pseudohomogeneous model where the chemical reactions are first order and irreversible [5, 21, 34], and the kinetic constants are respectively k_1 and k_2, can be considered.

The corresponding mass balances in the stirred batch reactor are:

$$\frac{dC_A}{dt} = \frac{W_{CAT}}{V_R}\left(-k_1 C_A\right) \quad C_{A(t=0)} = C_A^o = \frac{m^o}{MW_{TIPB}\, V_R} \qquad (1)$$

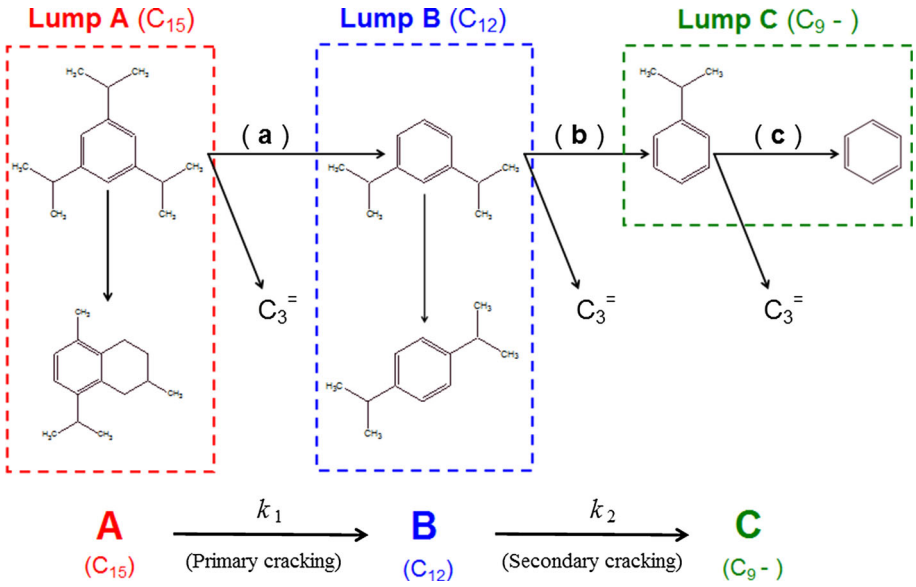

Fig. 7 Simplified reaction scheme for the conversion of TIPB over acidic catalysts

$$\frac{dC_B}{dt} = \frac{W_{\mathrm{CAT}}}{V_{\mathrm{R}}}\left(+k_1 C_A - k_2 C_B\right) \quad C_{B(t=0)} = 0 \tag{2}$$

$$\frac{dC_C}{dt} = \frac{W_{\mathrm{CAT}}}{V_{\mathrm{R}}}\left(+k_2 C_B\right) \quad C_{C(t=0)} = 0 \tag{3}$$

W_{CAT} is the mass of catalyst in the reactor (0.4 g), V_{R} is the reactor volume (0.45 cm^3), m^{o} is the mass of reactant injected (0.085 g) and $\mathrm{MW}_{\mathrm{TIPB}}$ is the molecular weight of the reactant (204 g/mol).

Experimental data analysis was performed by solving the mass balances, ordinary coupled differential equations by means of an algorithm based on an explicit Runge–Kutta (4–5) formula, and data fitting by a least squares method. The resulting parameters are shown in Table 6, where it can be seen that the values of the apparent overall kinetic constant k_1 are consistent with the observed activities for each catalyst (refer to Fig. 4).

The relative incidence of the secondary cracking reactions can be assessed by means of the relationship between k_2 and k_1, thus defining the secondary cracking index (i_{sc}) as:

$$i_{SC} = \frac{k_2}{k_1} \tag{4}$$

Table 6 Three lump model for the conversion of TIPB

	Cat-00	Cat-10	Cat-20
$k_1 \times 10^3$ (m^3/kg s)	1.02 ± 0.17	1.66 ± 0.16	1.55 ± 0.14
$k_2 \times 10^3$ (m^3/kg s)	11.10 ± 6.99	12.82 ± 5.00	8.74 ± 3.41

Apparent kinetic parameters at 500 °C

Figure 8 shows the i_{sc} values corresponding to the catalysts Cat-00, Cat-10 and Cat-20 calculated at the three reaction temperatures. It can be clearly observed that at a given temperature, the incidence of the secondary cracking decreased as a function of the mesoporosity induced in the zeolite component of the catalysts. This is consistent with the previous discussion about the observed product distributions, where it was stated that the increase in zeolite mesoporosity favors primary cracking reactions (refer to Fig. 5). Moreover, for each of the catalysts, i_{sc} increased as a function of the reaction temperature, a fact which can be ascribed to the typical higher impact of temperature on the chemical reactions as compared to diffusion processes (refer to Table 5). An immediate consequence is that the overall process becomes increasingly diffusion controlled and the secondary cracking is favored [36]. The same behaviours were observed by Tauster et al. [26] in the hydrocracking of hexanes over Pt–Ir/Al_2O_3 catalysts.

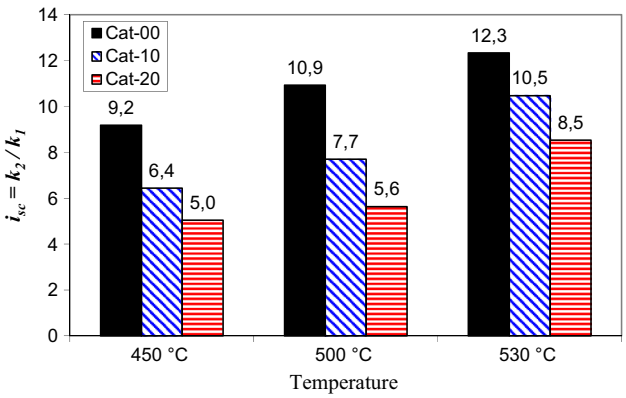

Fig. 8 Index i_{sc} (three lump kinetic model) as a function of reaction temperature for different catalysts

If a reaction A → C in a porous catalyst particle proceeds by way of an intermediary product B, it has been shown that the overall kinetics may be influenced by the diffusion transport rates of A into, and B and C out, of the particle pore system. That is, the diffusion transport rates of reactants and products within porous catalyst particles can significantly affect the interpretation of the observed (apparent) reaction rates and product distributions when more than a single one-step reaction proceeds [35]. The issue of diffusional effects on the selectivity of multiple reactions is of particular importance, with basic concepts provided by Wheeler [37] for different cases. It can be shown that diffusion limitations are the reason for the reduction of selectivity to the primary product in consecutive first-order reactions.

4 Conclusions

It is possible to modify the textural properties of USY zeolites, via desilication with alkaline lixiviation, in order to formulate compound catalysts such as those of FCC, increasing the contribution from mesopores in the range of 20–100 Å to the catalyst's specific surface area. The impact of the concentration of NaOH solutions in the alkaline desilication of zeolite on the formation of intracrystalline mesopores was studied and it was observed that the more severe the desilication treatment, the more mesoporosity was formed and the larger the mesopore size.

The use of 1,3,5-tri-isopropylbenzene as a model reactant representative of bulky hydrocarbon molecules allowed studying the influence of the increased mesoporosity in the Y zeolite over both its observed activity and the selectivities to the various reaction products. The increase in mesoporosity improved the observed cracking activity of the catalysts formulated with the modified zeolites, given the enhanced diffusion of the reactant molecules. Moreover, secondary cracking reactions had a lower incidence on the product distributions, since the products from primary cracking reactions could diffuse faster out of the catalyst pore system.

Acknowledgments This work was performed with the financial assistance of University of Litoral (Santa Fe, Argentina), Secretary of Science and Technology, Proj. CAID 2011 #501-201101-00546LI; The National Scientific and Technological Research Council, PIP 1257/09 and the National Agency for Scientific and Technological Promotion, PICT 2010/2123.

References

1. O'Connor P (2007) Catalytic cracking: the future of an evolving process. Stud Surf Sci Catal 166:227–251
2. Harding R, Peters A, Nee J (2001) New developments in FCC catalyst technology. Appl Catal A 221:389–396
3. Letzsch W, Ashton A (1993) The effect of feedstock on yields and product quality. Stud Surf Sci Catal 76:441–498
4. Al-Khattaf S, de Lasa H (2002) The role of diffusion in alkylbenzenes catalytic cracking. Appl Catal A 226:139–153
5. Al-Khattaf S, Atias J, Jarosch K, de Lasa H (2002) Diff-usion and catalytic cracking of 1,3,5 tri-iso-propyl-benzene in FCC catalysts. Chem Eng Sci 57:4909–4920
6. Martinez C, Verboekend D, Pérez-Ramírez J, Corma A (2012) Stabilized hierarchical USY zeolite catalysts for simultaneous increase in diesel and LPG olefinicity during catalytic cracking. Catal Sci Technol 3:972–981
7. Falabella Souza-Aguiar E, Murta Valle M, Silva M, Silva D (1995) Influence of external surface area of rare-earth containing Y-zeolites on the cracking of 1,3,5-triisopropylbenzene. Zeolites 15:620–623
8. Na K, Choi M, Ryoo R (2013) Recent advances in the synthesis of hierarchically nanoporous zeolites. Microporous Mesoporous Mater 166:3–19
9. Corma A, Diaz-Cabañas M, Jordá J, Martínez C, Moliner M (2006) High-throughput synthesis and catalytic properties of a molecular sieve with 18- and 10-member rings. Nature 443:842–845
10. Tonetto G, Atias J, de Lasa H (2004) FCC catalysts with different zeolite crystallite sizes: acidity, structural properties and reactivity. Appl Catal A 270:9–25
11. Gayubo A, Alonso A, Valle B, Aguayo A, Bilbao J (2010) Selective production of olefins from bioethanol on HZSM-5 zeolite catalysts treated with NaOH. Appl Catal B 97:299–306
12. Janssen A, Koster A, de Jong K (2002) On the shape of the mesopores in zeolite Y: a three-dimensional transmission electron microscopy study combined with texture analysis. J Phys Chem B 1067:11905–11909
13. de Jong K, Zečević J, Friedrich H, de Jongh P, Bulut M, van Donk S, Kenmogne R, Finiels A, Hulea V, Fajula F (2010) Zeolite Y crystals with trimodal porosity as ideal hydrocracking catalysts. Angew Chem Int Ed 49:10074–10078
14. Groen J, Moulijn J, Pérez-Ramírez J (2007) Alkaline posttreatment of MFI zeolites. From accelerated screening to scale-up. Ind Eng Chem Res 46:4193–4201
15. Verboekend D, Vilé G, Pérez-Ramírez J (2012) Mesopore formation in USY and beta zeolites by base leaching: selection criteria and optimization of pore-directing agents. Cryst Growth Des 12:3123–3132
16. Verboekend D, Keller T, Mitchell S, Pérez-Ramírez J (2013) Hierarchical FAU- and LTA-type zeolites by post-synthetic design: a new generation of highly efficient base catalysts. Adv Funct Mater 23:1923–1934
17. García JR, Bertero M, Falco M, Sedran U (2015) Catalytic cracking of bio-oils improved by the formation of mesopores by means of Y zeolite desilication. Appl Catal A 503:1–8
18. Hartmann M (2004) Hierarchical zeolites: a proven strategy to combine shape selectivity with efficient mass transport. Angew Chem Int Ed 43:5880–5882
19. Groen J, Zhu W, Brouwer S, Huynink S, Kapteijn R, Moulijn J, Pérez-Ramírez J (2007) Direct demonstration of enhanced diffusion in mesoporous ZSM-5 zeolite obtained via controlled desilication. J Am Chem Soc 129:355–360
20. Jiménez-García G, Aguilar-López R, Maya-Yescas R (2011) The fluidized-bed catalytic cracking unit building its future environment. Fuel 90:3531–3541
21. Tukur N, Al-Khattaf S (2005) Catalytic cracking of n-dodecane and alkyl benzenes over FCC zeolite catalysts: time on stream and reactant converted models. Chem Eng Process 44: 1257–1268
22. Bazyari A, Khodadadi A, Hosseinpour N, Mortazavi Y (2009) Effects of steaming-made changes in physicochemical properties

of Y-zeolite on cracking of bulky 1,3,5-triisopropylbenzene and coke formation. Fuel Process Technol 90:1226–1233
23. Falco M, Morgado E, Amadeo N, Sedran U (2006) Accessibility in alumina matrices of FCC catalysts. Appl Catal A 315:29–34
24. Morales-Pacheco P, Domínguez J, Bucio L, Alvarez F, Sedran U, Falco M (2011) Synthesis of FAU(Y)- and MFI(ZSM5)-nanosized crystallites for catalytic cracking of 1,3,5-triisopropylbenzene. Catal Today 166:25–38
25. Aghakhani M, Khodadadi A, Najafi Sh, Mortazavi Y (2014) Enhanced triisopropylbenzene cracking and suppressed coking on tailored composite of Y-zeolite/amorphous silica–alumina catalyst. J Ind Eng Chem 20:3037–3045
26. Tauster S, Ho T, Fung S (1987) Assessment of diffusional inhibition via primary and secondary cracking analysis. J Catal 106:105–110
27. Emeis C (1993) Determination of integrated molar extinction coefficients for infrared absorption bands of pyridine adsorbed on solid acid catalysts. J Catal 141:347–354
28. Renzini MS, Sedran U, Pierella L (2009) H-ZSM-11 and Zn-ZSM-11 zeolites and their applications in the catalytic transformation of LDPE. J Anal Appl Pyrolysis 86:215–220
29. de Lasa H (1992) Novel Riser simulator reactor. US Patent 5.102.628
30. de la Puente G, Sedran U (2004) Formation of gum precursors in FCC naphthas. Energy Fuels 18:460–464
31. de la Puente G, Ávila A, Chiovetta G, Martignoni W, Cerqueira H, Sedran U (2005) Adsorption of hydrocarbons on FCC catalysts under reaction conditions. Ind Eng Chem Res 44:3879–3886
32. Sullivan R, Egan C, Langlois G (1964) Hydrocracking of alkylbenzenes and polycyclic aromatic hydrocarbons on acidic catalysts. Evidence for cyclization of the side chains. J Catal 3:183–195
33. Gilbert W, Morgado E, de Abreu M, de la Puente G, Passamonti F, Sedran U (2011) A novel fluid catalytic cracking approach for producing low aromatic LCO. Fuel Process Technol 92:2235–2240
34. Wojciechowski B, Corma A (1986) Catalytic cracking. Catalysts, chemistry, and kinetics. Marcel Dekker, New York
35. Weisz P, Swegler E (1955) Effect of intra-particle diffusion on the kinetics of catalytic dehydrogenation of cyclohexane. J Phys Chem 59:823–826
36. Kärger J, Ruthven D (1992) Diffusion in zeolites and other microporous solids. Wiley, New York
37. Froment G, Bischoff K, De Wilde J (2011) Chemical reactor analysis and design. Wiley, New York